Characterization of Laser Induced Charging Damage in Laser Micromachining

Jong-Souk Yeo

Hewlett-Packard Company, 1000 NE Circle Boulevard, Corvallis, Oregon, 97330, USA
E-mail: jong-souk.yeo@hp.com

Laser induced damage has been observed from laser micromachining of Si with insulating material on device structures. Characterization of damage suggests the potential mechanism as laser induced charging damage. Static measurements using a Langmuir type probe for measuring average spatial charge distributions, accumulated charges, and maximum current are conducted to understand the charge characteristics of laser micromachining on Si and on insulating layer/Si. The amount of charge accumulating on the probe is seen to be proportional to the increase in laser energy, repetition rate, spatial overlap, and probe bias. Machining of insulating layer coating on Si shows the accumulation of positive charge while machining of bare Si indicates cumulative small positive or negative charges depending on the location of the probe. Hydrofluorocarbon (HFC) assisted ablation generates an order of magnitude smaller amount of charge compared to no assist ablation. Spatial charge profiles show a rapidly decaying distribution with distance away from ablation region and a fit of these data to a $\cos^n\theta$ function shows an increasing value of n as a function of distance from the wafer surface.

DOI: 10.2961/jlmn.2007.01.0013
Keywords: laser induced damage, laser micromachining, probe, laser induced charging

1. Introduction

Laser micromachining is increasingly utilized for industrial applications in semiconductor processing. One of the major applications is in the area of thru-slotting process for ink-jet printing. While laser micromachining is a useful production technique, it can cause laser induced damages to component layers positioned on a substrate during laser processing with debri generation, heat damage, and microcracks. Newer type of laser induced damage is observed where the laser micromachining is applied to a specific combination of material sets defined on microelectronic device. The detailed mechanism of this process is complex due to the temporal and spatial nature of laser-material interaction as well as its dependence on the set of material combinations but the characterization of the laser induced damage in laser micromachining indicates a laser induced electro-static-discharge as the potential mechanism. For plasma induced charging damage (PID) in semiconductor processing, there have been many studies as the thickness of gate oxide decreases [1-3] but the report on the laser induced charging damage with nanosecond pulses is yet to be seen. It is mainly because nanosecond laser machining is at the early stage of adoption in industrial application and mostly used for bare substrate materials. Laser induced plasma itself has been intensely studied for the deposition and spectroscopic application where diagnostics are focused mostly on optical or x-ray probing [4]. Surface charging due to the femtosecond pulses with impulsive Coulomb expulsion has been investigated for ultrashort pulsed laser ablation [5]. Mechanism of charge collection in semiconductor devices with picosecond laser pulse has been studied with probing circuits [6].

Laser induced charging damage occurs when highly insulating layers with conductive structures are present in laser ablation process where laser induced charges can not effectively dissipate. The electrical breakdown caused by the break-thru interaction of laser with a dielectric film damages underlying resistors and other related areas. Since the laser plasma generates significant number of charges within a very short interaction time and the charges are contained fairly locally where the ablation occurs and the subsequent plume expands, the rate of charge accumulation can be extremely high if the charges are not dissipated efficiently and the pulses rapidly overlap within the lifetime of charge carriers that depend on ambient conditions. The measurement of the charge distribution where laser breaks through the silicon may directly provide information necessary to understand laser-induced electrical breakdown. But it may not be feasible to measure the electrical characteristics in real time due to short duration, high directionality, and non-steady state behavior of laser induced plasma. Also placing probe within the plasma can affect probe characteristics since laser can damage the probe and interfere with the measurement by generating photoelectrons or by depositing Si species on the probe. Regardless, the probe placed near the ablated region still provides useful information by collecting the fluxes of charges diffusing through ambient to reach the probe.

We have used a Langmuir type probe to measure the average spatial charge distributions, accumulated charges for the duration of slotting process, and maximum current during the laser ablation of Si. Along with probe analysis, physical characterization of laser induced damage is discussed to explain the possible mechanism of the laser induced damage in the laser micromachining process. Figure 1 shows the top and cross-sectional scanning electron micrograph of the damaged regions during laser micromachining process.

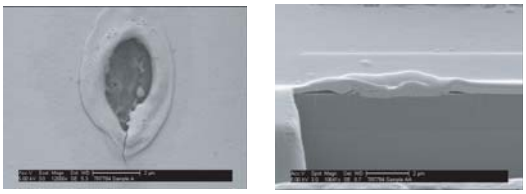

Fig. 1 Top and cross-sectional view of laser induced damage.

2. Experimental Set Up

For a steady state plasma, a Langmuir probe measurement, where an electrically isolated probe is placed in the plasma with a potential set by an external power source, can provide parameters such as electron and ion temperatures, plasma density, and plasma potential [7]. Temporal behavior of a plume has been measured with time-resolved Langmuir probe in vacuum [8]. In this experiment, we are interested in an average cumulative response from overlapped pulses during laser machining in various ambient conditions rather than a diagnostic of a single plume. Simple probe is used to measure net charges from electrons and ions arriving at the probe with different densities (cumulative charge) and velocities (rate of charge accumulation) for the duration of slotting process. Charges initially interact within expanding plume, followed by an interaction with ambient species through multiple collision processes. For example, when each laser pulse removes about 3,000 μm^3 in the ablation of Si (with atomic density of 5×10^{22} cm^{-3} or 5×10^{10} μm^{-3}), it is expected to generate 1.5×10^{14} species. Depending on the ionization rate of neutral species ($\sim10^{-4}$ % to ~10 %), number of ions and electrons generated for each pulse can vary from 10^8 to 10^{13}. With 55,000 Hz of repetition rate for laser pulses, the range can become 10^{13} to 10^{16} per second. Though high density of plasma species are generated with laser ablation process, this is within the plume and most of those charged species are lost by redeposition to side walls and relaxation through recombining with the charges available in the ambient. We can only collect fluxes of charges diffusing through ambient to reach the probe without being lost in that process.

In order to capture small amount of charges generated from laser induced plasma, Keithly Electrometer with the resolution of pC and pA is used for the charge and current measurement respectively. As shown in Fig. 2, Langmuir probe on x-y translational stage is placed near ablated region from the substrate surface. Probe is made of a needle and connected to Electrometer that can provide positive and negative bias relative to the ground. As the plasma duration for pulsed ablation is very short to detect appreciable amount of charges and our objective is to understand the surface charge build-up during laser slotting process, a generic slotting program is used for the measurement of charges accumulated for the duration of 15 seconds during laser slotting process. For laser micromachining, third harmonic generated 355 nm solid state laser is used with Galvo scanning head. Rate of accumulation continues to decrease as the laser ablates deeper into a slot so that distance between plume and probe increases. Current measurement indicates maximum value at the onset of ablation since the highest rate of charge accumulation occurs from launching hot electrons ahead of the main body of the plume [8].

The probe measurement in this report is not done from the backside of wafer as in the situation with laser induced damage since 1) charge flux is only generated at the time of break-thru for a very short time making the determination of probe position difficult, 2) alignment of each die requires wafer chuck to move constantly, which prevents probe from being set up at the backside, and 3) charge flux generated from the other side is expected to be order of magnitude smaller than the front side due to the directionality of plume. Instead, spatial profiles of charge and current distribution are obtained using laser micromachining from either bare Si or Si wafer coated with 10 um thick polyvinyl alcohol (PVA) to see the effect of an insulating layer on the surface charge accumulation. Poly vinyl alcohol (C_2H_4O) is a water soluble polymer with a high dielectric constant. The electrical properties of PVA is reported and discussed by other researchers in detail [9-11].

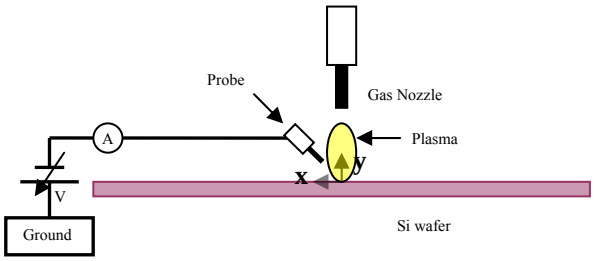

Fig. 2 Schematics of the probe measurements for a laser-induced plasma

3. Results

3.1 Effect of Laser Energy

As laser fluence changes, the amount of material removed is expected to change, which affects the number of charges generated in the ablation process. The following Table 1 shows the values of energy and corresponding diode pump current used in the experiment.

Table 1 Laser parameters and charge measured in experiment.

Current (%)	Pulse Energy (μJ)	Fluence (J/cm^2)	Qaccum (nC)
80	8.4	1.2	0.004
85	22	3.1	0.003
87	38	5.4	0.039
90	75	10.6	0.553
92	110	15.6	0.946
94	126	17.8	1.271

Laser is operated at 60 kHz and the probe is located at x = 0.25 mm, y = 1.4 mm and the charge is accumulated over a time of single slotting process. It is interesting to note that the surface charges indicate an accumulation of positive charges from the ablation of PVA/Si side. From the Electrometer panel, it is observed that the initial surge of negative charges is followed by larger amount of positive charges that keep accumulating to the end of slotting process, though the rate of accumulation decreases as ablated region moves away from probe going deeper into the slot. Contribution of PVA on the charges themselves is expected

to be minimal as PVA is rapidly removed by laser ablation and the subsequent ablation is dominated by Si-laser interactions. While Si surface can provide effective dissipation path for electrons, insulating PVA coating is believed to delay the relaxation of spatial charges, thus accumulating charges on the surface.

From Table 1, we can plot a relationship between the cumulative charge and the fluence as shown in Fig. 3. This experiment is done with the ambient condition of HFC with the flow rate of 0.5 standard cubic feet per hour (SCFH). Fluence indicates the average number of photons interacting with atoms on the surface area defined by the laser beam. Once the fluence reaches over the ablation threshold, surface charges increase linearly with increasing fluence.

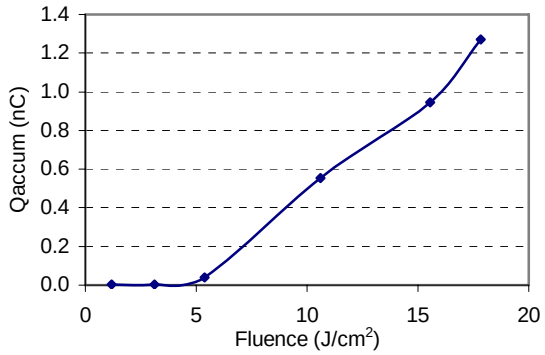

Fig. 3 Effect of laser fluence on cumulative charges in the probe.

3.2 Effect of Overlap

Amount of linear overlap (o) between the pulses is determined by the diameter of beam (d) subtracted by the distance traveled given by the scan rate (v) multiplied by the interval (1/f) between the pulses. (d - o = v/f) Therefore, increasing overlap means either decreasing the scan rate of Galvo mirror or increasing the repetition rate of a laser pulse. Since laser energy inherently changes with varying repetition rate, we need to adjust diode pump current to maintain per-pulse laser energy at the same level in order to separate the effect of laser fluence on surface charge profile. For this experiment, the fluence is maintained at 17.8 J/cm^2, the scan rate is 120 mm/sec, and the ambient condition is with HFC gas with the flow rate of 0.5 SCFH. Table 2 shows the values of repetition rate and corresponding overlap changes with cumulative charges measured at the probe located at x = 0.25 mm, y = 1.4 mm.

Table 2 Repetition rate, overlap parameters, and charges measured in the experiment.

Current (%)	Repetition Rate (kHz)	Overlap (%)	Qaccum (nC)
89.3	30	86.7	-0.065
90.3	40	90.0	-0.089
91.3	50	92.0	-0.121
94	60	93.3	-0.145

This experiment is conducted on Si in order to see the effect of bare Si without insulating layer on it. For similar location of the probe, Si side ablation tends to accumulate negative charges on the probe compared to positive charges from the ablation of PVA coating on Si. The negative value increases linearly with increasing repetition rate or increasing overlap as shown in Fig. 4.

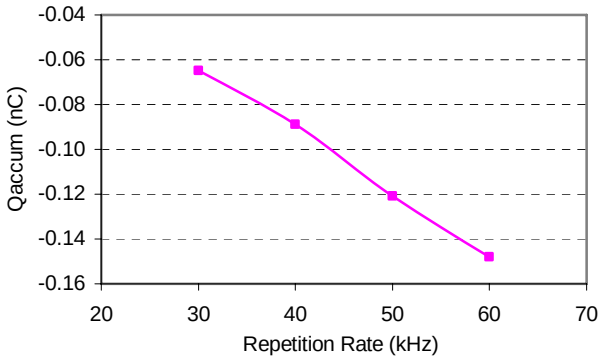

Fig. 4 Effect of laser repetition rate on the cumulative charges on the probe.

This net cumulative charge for the duration of slotting process is a result from the flux of charges arriving at the probe. The numbers of electrons and ions should be same at the time of generation inside plume. But in Si ablation, higher number of electrons arrives at the probe due to their higher velocities while some of the ions are apparently lost in the ablation process. The location of the probe is same for the experiments on the ablations of Si and PVA/Si. Net charge (Δn) is the difference between the number of ions (n_i) and electrons (n_e). At the repetition rate of 60 kHz and the fluence of 17.8 J/cm^2, PVA/Si machining gives the net number of accumulated charges as $1.271\times10^{-9}/1.602\times10^{-19} = 7.93\times10^{9}$ while in Si machining, net number of charge is $-0.145\times10^{-9}/1.602\times10^{-19} = -0.91\times10^{9}$. From the following,

$$\Delta n = n_i - n_e \text{ (PVA/Si)} = 7.93\times10^{9} \quad (1)$$

$$\Delta n = n_e \text{ (bare Si)} - n_i = 0.91\times10^{9} \quad (2)$$

$$(1) + (2) = n_e \text{ (bare Si)} - n_e \text{ (PVA/Si)} = 8.84\times10^{9} \quad (3)$$

Adding (1) and (2) gives us the amount of electrons (8.84×10^{9}) lost for the machining of PVA coating on Si device structure compared to that of Si substrate alone. This result suggests that the conductive layers from a thin film side with PVA coating may capture some of the electrons before they leave Si wafer diffusing into ambient gas, which potentially causes the charges to build up on the surface with remaining balance of positive ions.

3.3 Effect of Probe Bias

Bias applied to the probe can prevent electrons or ions from reaching the probe depending on the polarity of bias. In steady state plasma with a fixed number of ions and electrons, saturation current density exists for a bias larger than certain value where respective charges are completely suppressed. In our experiments, we do not observe this as laser induced plasma is in non-steady state and the probe is not submerged in a plume. The charge density inside plume is fairly high so that spatially dispersed charges can continue to be drawn to the probe as the bias is increased. Fig. 5 shows the plot of maximum current vs voltage applied to

the probe for the plasma generated from the machining of Si with the probe position of x = 1 mm, y = 4 mm at the laser repetition rate of 60 kHz and the pump current at 94%. With the onset of ablation process, current rapidly reaches maximum value and fluctuates to stabilize to a finite small value over the course of micromachining process. This is related to the rate of charge accumulation with hot electrons and the remaining charges as explained before. For this experiment, only the maximum current is recorded as that is what may initiate laser-induced electrostatic discharge.

The noticeable difference is the amount of charges created in the process with and without HFC gas. Without the gas assist process, the rate of charge accumulation seems to be an order of magnitude higher in the micromachining with air ambient. This indicates that the charges are lost in the gas assist process. It is proposed that Si ions are lost by combining with the fluorine decomposed from HFC and turning into a volatile silicon fluoride gas. This needs further investigation in correlation to the mechanism of HFC gas assist process. When there is no ablation, probe still draws some current from air with bias but at negligible noise level of couple pA. The graph shows that both cases show positive floating potential on the probe (+1.3 V with HFC and +2.2 V with air) without bias since energetic ions with larger mass may diffuse further away from the ablated region and the gas layer between distributed charges and wafer may serve as insulating layer for those to dissipate promptly.

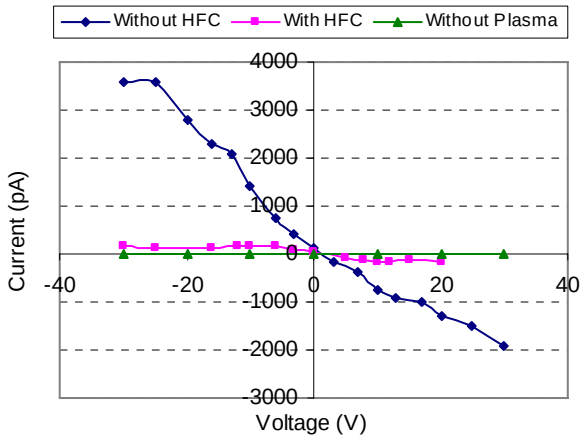

Fig. 5 Effect of probe bias on the current measured in a probe.

3.4 Effect of Thin Film Side with PVA coating

As briefly discussed before, varying bias condition in air clearly indicates the effect of thin film side with PVA coating on the build-up of positive charges compared to bare Si side. Fig. 6 shows the net charge concentration profile with the probe position at y = 1.4 mm with varying x away from the ablated region on the bare Si and PVA/Si substrate respectively. This indicates the effect of insulating layer on the charge balance from laser induced plasma. When the probe is in contact with a Si surface, the values measured at y = 0 fluctuates from a negative near the ablated region (-0.75 nC at x = 0.5 mm) to a positive away from slot (+93.1 nC at x = 3 mm).

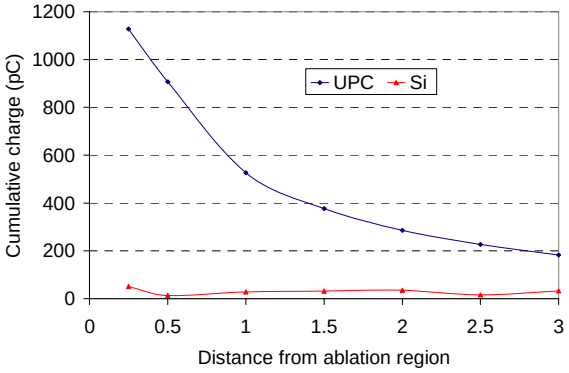

Fig. 6 Cumulative charge distribution with the probe for bare Si surface and thin film side with PVA.

Fig. 7 shows how cumulative charges vary with the probe bias for different surface conditions when surface is ablated in the air (probe position at x = 0.25 mm, y = 1.4 mm). At 0 bias, the probe on Si side charges up negatively (-2.92 nC) while the probe on PVA side charges up positively (+1.21 nC). It seems that the electrons generated in the ablation process from the thin film side with PVA are dissipated more than the electrons from Si side. It is interesting to note that electrons on PVA side can be drawn even more than the ones on Si side for bias larger than 10 V.

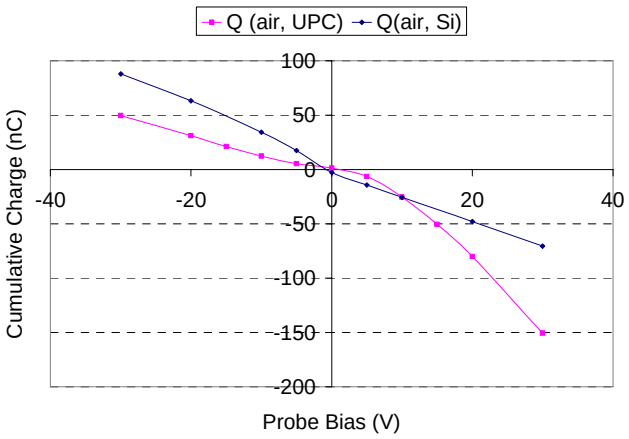

Fig. 7 Cumulative charge vs probe bias for the bare Si surface and the thin film side with PVA.

3.5 Effect of Ambient Gas

As discussed earlier, ionization rate with air seems to be order of magnitude higher than that with HFC. Experiment is conducted to measure the charge accumulation at the probe (x = 0.25 mm, y = 1.4 mm) in the ambient gas condition of air and HFC when the surface is ablated from the thin film side with PVA. From this, we can expect to see electro-static discharge (ESD) damage from the ablation in air ambient if we see damage with HFC gas assist in a given condition. Once the amount of charge is over the critical value to initiate ESD, extra amount of charges is not expected to cause more damage as they can be relieved through the path previously opened up with the electrical breakdown. But for the higher amount of charges with air

ambient, the probability of supplying critical density of charges further away from the ablated region may increase so that breakdown condition can be satisfied at a larger distance.

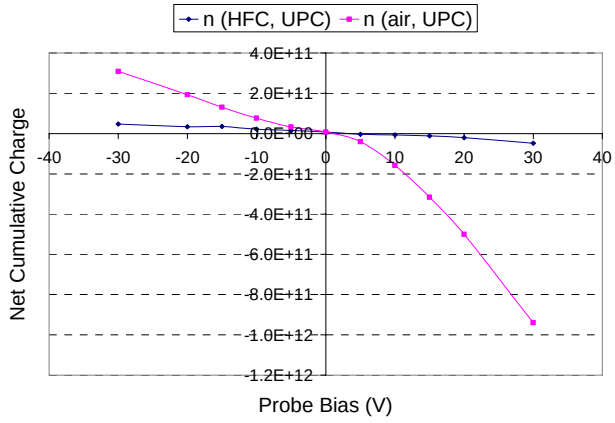

Fig. 8 Cumulative charge vs probe bias in HFC and air on PVA.

3.6 Spatial Charge Profile

Spatial profiles of cumulative net charge and maximum current are measured for the varying probe position with the ablation condition of HFC on thin film side with PVA. Spatial profile shows the energy and density of species diffused through nearby area where the plume expands. Plume is expanding directly parallel to y axis shown in the graph and along x axis at the same time. Dynamics of the charged species within a plume is dominated by an initial energy supplied to the species at the time of ablation and the interactions among the species within a boundary relatively defined between the plume and the ambient gas. As that boundary breaks apart through the ambient gas when plume expands, plasma species are expected to stagnate and start to drift away by interacting with the surrounding gas species depending on the driving force set by concentration, energy, and charge gradients. Steady state ionization rate within the plasma and charge recombination rate for ions and electrons traveling out to the probe determine the net charge accumulation for the duration of single slotting process. The maximum current which is the indication of fastest rate of charge accumulation occurs at the onset of laser ablation where the distance from the ablated region to the probe is shortest. As laser ablates deeper into a slot, charged species have to drift additional distance to reach the probe and they may dissipate in that process.

Fig. 9 shows spatial charge profiles that indicate how species are distributed from the plume located along y axis at x = 0. Clearly the plume expands vertically to the surface and spreads out to the side. Cumulative charge profiles show mostly positive value except at the surface far away from the plume for the case of thin film side ablation with PVA. Fig. 10 shows spatial maximum current profiles which show similar trend with cumulative charge. Based on the data from Fig. 9, we can calculate the number of net charges detected at a probe, which shows the distribution of uncompensated charges on the wafer surface. This distribution can be fitted with well-known cosine distribution for laser ablation ($\cos^n\theta$ where θ is an angle increasing from surface normal). Due to the directionality of an expanding plume, n value is usually very large depending on laser and material parameters. Since the amount of material ejected in the ablation process is responsible for the amount of charged species, the distribution of the net cumulative charge is also expected to follow the characteristic spatial profile created by laser ablation. The value of n may be different between those two distributions depending on the charge dynamics in the ambient.

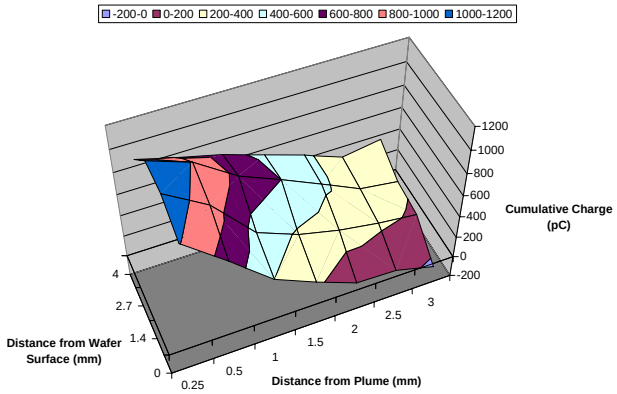

Fig. 9 Cumulative spatial charge profile.

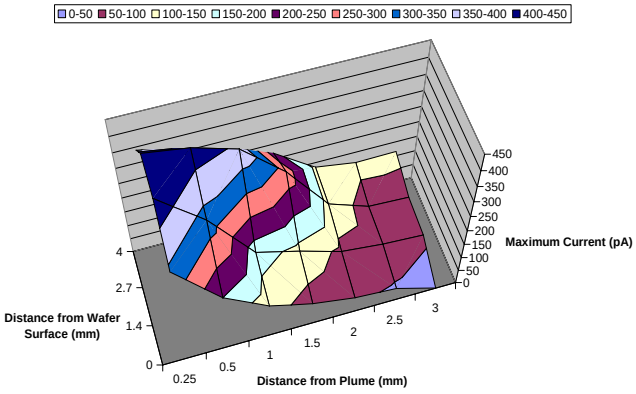

Fig. 10 Spatial maximum current profile.

Fig. 11 shows that charge concentration rapidly decreases along y axis as it gets closer to the surface. The plot in Fig. 12 shows this trend of n increasing from ~4 to ~17 as the probe gets closer to the wafer surface.

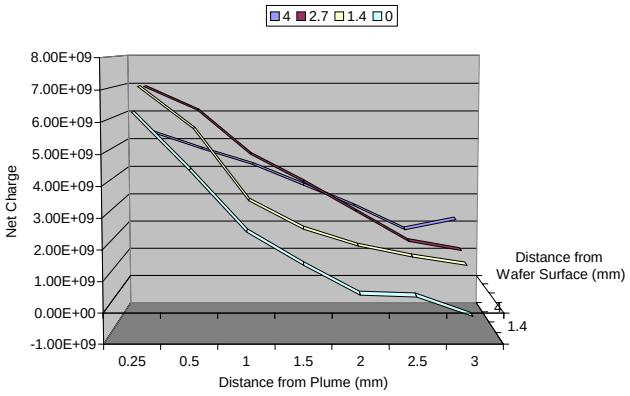

Fig. 11 Distribution of net cumulative charge.

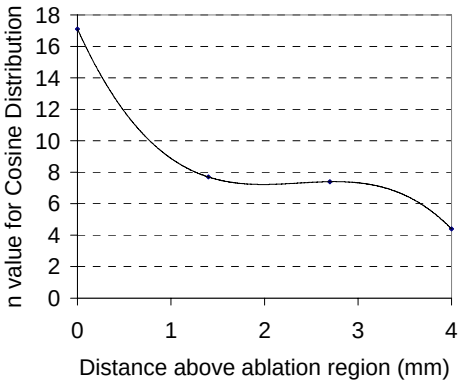

Fig. 12 Trend plot of n value fitted for cosine distribution.

4. Discussion

From all the measurements involved in this experiment, we have identified what laser parameters do in terms of localized charge accumulation. As expected, the amount of charges and the rate of accumulation depend on the amount of materials removed and how fast those materials are removed. Laser beam is expected to evaporate materials and instantly create plasma by dissociating species into charged particles, ions, electrons, and neutrals. Though absolute value presented in this experiment is not an indication of any absolute measures for the laser-induced plasma, the percent increase or decrease in the cumulative charges, maximum currents, or the rates of charge accumulation with changing condition of laser parameters, ambient gas, and substrate conditions is meaningful and important since they represent what is happening within or close to a laser-induced plume during laser micromachining process.

As long as we maintain the probe position constant, the probability of charged species reaching the probe should remain constant for the ions and electrons, respectively with the given condition of plasma generation and ambient. Also, the measurement is done from the side where laser beam ablates since it is difficult to measure from back side at the time of break-thru. It is expected that a flux from the back side at the break-thru should be fairly small compared to the flux on the front because of the directionality during plume expansion. But there are a couple of potential mechanisms that may suggest higher flux than we may expect from this directionality argument.

When a laser opens up the hole, high pressure plume can expand through that hole after the initial break-thru due to the pressure difference or the interaction with shock wave. Also, the charged species can be accelerated through Inverse Bremsstrahlung process by interacting with high intensity laser beam directed out of break-thru spot. At the time of break-thru, inner wall of the machined region can form a slope that reflects and redirects the part of incoming beam through the break-thru region rendering a secondary ablation depending on the intensity of reflected beam.

Even with the various mechanisms associated with the charge generation on the backside, it is certain that we will have a concentration profile that rapidly decreases at a distance so the proximity of dissipation path to relieve electrostatic charges is an important factor to consider. Depending on the combinations of materials and device structures, we have seen the damages over 100 um away from the ablated region and on thin film topography parallel to the slot edge.

5. Summary

We have used a Langmuir type probe to measure the spatial charge distributions, accumulated charges, and maximum currents during the laser micromachining of Si. The amount of charges accumulating on the probe for the duration of slotting process is proportional to the increase in laser energy, repetition rate, spatial overlap, and probe bias. Thin film side with PVA coating shows the accumulation of positive charge while the ablation of bare Si side indicates cumulative small positive or negative charges depending on the location of the probe. HFC assisted ablation generated an order of magnitude smaller amount of charges compared to no assist ablation. Spatial charge profiles show rapidly decaying distributions with the distance away from the ablated region. The value of n in fitted cosine distributions increases as the probe gets close to the wafer surface. Along with probe analysis, physical characterization of the laser induced damage is discussed to explain the possible mechanism of the laser induced damage in laser micromachining process.

Acknowledgments and Appendixes

Author would like to acknowledge the contributions from Mark Huth, Mehrgan Khavari, Laura King, Sean McClelland, Seamus O'Brien, Chuck Otis, Sue Richards, Phil Rourke, Graeme Scott, and Analytical and Development Lab at HP Corvallis. This work was mostly conducted at the Advanced Materials and Processes Lab at HP Corvallis.

References

[1] K. P. Cheung and C. P. Chang: J. Appl. Phys., **75**, (1994) 4415.

[2] H. Shin, K. Noguchi, and C. Hu: IEEE Dev. Lett., **14**, (1993) 509.

[3] K. Hashimoto: Jpn. J. Appl. Phys., **32**, (1993) 6109.

[4] A. A. Hauer and H. A. Baldis: "Laser-Induced Plasmas and Applications ed. by L. J. Radzienski and D. A. Cremers, (CRC, 1989) p.105.

[5] R. Stoian, A. Rosenfeld, D. Ashkenasi, I. V. Hertel, N. M. Bulgakova, and E. E. B. Campbell: Phys. Rev. Lett., 88, (2002) 097603.

[6] J. S. Melinger, D. McMorrow, A. B. Campbell, S. Buchner, L. H. Tran, A. R. Knudson, and W. R. Curtice: J. Appl. Phys., **84**, (1998) 690.

[7] N. Hershikowitz: "Plasma Diagnostics" ed. by O. Auciello, D. L. Flamm, (Academic, Boston, 1989), Chap. 3

[8] Z. Zhang, P. A. VanRompay, J. A. Nees, and P. P. Pronko: J. Appl. Phys., **92**, (2002) 2867.

[9] B. C. Shekar, V. Veeravazhuthi, S. Sakthivel, D. Mangalarai, and S. K. Naravandass, Thin Solid Films, **348**, (1999) 122.

[10] S. H. Jin, J. S. Yu, C. A. Lee, J. W. Kim, B. G. Park, and J. D. Lee, J. Kor. Phys. Soc., **44**, (2004) 181.

[11] X. Z. Peng, G. Horowitz, D. Fichou, and F. Garnier, Appl. Phys. Lett., **57**, (1990) 2013.

(Received: May 16, 2006, Accepted: February 20, 2007)